Research Square

Preprints are preliminary reports that have not undergone peer review.
They should not be considered conclusive, used to inform clinical practice,
or referenced by the media as validated information.

Fast Prediction of Aero-Thermal Performance During Hypersonic Vehicle Design

Vinícius Hagemeyer Chiumento

vini.hagemeyer@gmail.com

Institute for Advanced Studies

Pedro Paulo Batista de Araújo

Institute for Advanced Studies

Fábio Henrique Eugênio Ribeiro

Institute for Advanced Studies

Angelo Passaro

Institute for Advanced Studies

Lucas Galembeck

Institute for Advanced Studies

Johan Steelant

European Space Agency

Research Article

Keywords: Aerothermodynamics, Heat transfer, Aerodynamics

Posted Date: July 6th, 2026

DOI: https://doi.org/10.21203/rs.3.rs-9998737/v1

License: This work is licensed under a Creative Commons Attribution 4.0 International License.
Read Full License

Additional Declarations: No competing interests reported.

Fast Prediction of Aero-Thermal Performance During Hypersonic Vehicle Design

Vinícius Hagemeyer Chiumento[1*],
Pedro Paulo Batista de Araújo[1†],
Fábio Henrique Eugênio Ribeiro[1†], Angelo Passaro[1†],
Lucas Galembeck[1†], Johan Steelant[2†]

[1*]Institute for Advanced Studies, Trevo Coronel Aviador José Alberto Albano do Amarante 1, São José dos Campos, 12245-021, São Paulo, Brasil.
[2]European Space Agency (ESTEC), Keplerlaan 1, City, 2201AZ, Noordwijk, The Netherlands.

*Corresponding author(s). E-mail(s): vini.hagemeyer@gmail.com;
Contributing authors: araujo.projects@gmail.com;
henriquefher@fab.mil.br; angelopassaro@gmail.com;
galembecklg@fab.mil.br; Johan.Steelant@esa.int;
†These authors contributed equally to this work.

Abstract

HipeX is a fast and lightweight aerothermodynamic analysis tool developed to estimate aerodynamic coefficients and surface heat fluxes on hypersonic vehicles using local surface inclination methods. The solver combines classical techniques such as the tangent-wedge method, the modified Newtonian approach, and Prandtl–Meyer expansions to evaluate pressure distributions across arbitrary geometries. Heat flux predictions are derived using similarity-based boundary-layer models, with compressibility effects accounted for through Eckert's reference temperature formulation. A key feature of HipeX is its blended boundary-layer model, which transition from laminar to turbulent flow based on local Reynolds number. Evaluation with CFD data for the HEXAFLY-INT experimental configuration shows that HipeX provides reliable aerodynamic and thermal load estimates.

Keywords: Aerothermodynamics, Heat transfer , Aerodynamics

1 Introduction

Local surface inclination methods are of significant importance in the design of hypersonic vehicles, as they provide rapid and reasonably accurate estimations of aerodynamic forces and heat transfer. These methods enable swift design iterations and optimizations during the early stages of development, when detailed computational fluid dynamics (CFD) simulations can be prohibitively time-consuming.

Local surface inclination methods have long been employed in hypersonic vehicle design as rapid tools for estimating aerodynamic loads during early development stages, when high-fidelity CFD analyses are computationally prohibitive. Classical approaches such as the tangent-wedge method, modified Newtonian theory, and Prandtl–Meyer expansions have been extensively used to capture inviscid flow features around complex geometries with reasonable accuracy [1] [2].To address this limitation, viscous contributions are typically introduced through boundary-layer similarity solutions, using correlations derived for flat-plate flows aligned with local streamlines. The boundary layer is then assumed either fully laminar or fully turbulent. Although the turbulent assumption offers a conservative estimate, it often overpredicts skin-friction drag and surface heat flux, leading to oversized thermal protection systems and increased vehicle mass and fuel consumption [3] [4]. More recent studies have highlighted the importance of accurately modeling boundary-layer transition in hypersonic flows, as transitional effects can significantly alter both aerodynamic and thermal loads [5]; however, only a few fast engineering-level tools have incorporated such effects within local-inclination frameworks.

This paper presents recent improvements to a computational tool named HipeX for aerodynamics and heat transfer analysis using local surface inclination methods [6] [7]. To enhance the fidelity of the physical model, transitional boundary layer modeling is employed. In this approach, a critical Reynolds number is calculated to determine the onset of transition from laminar to turbulent flow. The surface is then modeled using a composite approach, combining laminar and turbulent boundary layer characteristics over a defined transition region [5]. This methodology directly influences system-level metrics such as structural mass, insulation thickness and fuel margin. Incorporating transition effects is therefore essential for optimizing vehicle performance and achieving a balanced trade-off between design conservatism and mission efficiency.

2 Methodology

The HipeX computational program implements a set of computationally inexpensive models adapted from the literature. The program determines aerodynamic coefficients through a hybrid engineering-level approach by selectively applying the most appropriate model, such as tangent-wedge, modified Newtonian, or Prandtl-Meyer expansion, depending on the local surface inclination relative to the incident velocity vector.

The HipeX computational procedure begins by loading a 3D model and a set of flight conditions, including Mach number, altitude, angle of attack (AoA), and sideslip angle (AoS). For each condition, HipeX computes inviscid surface properties, such as pressure and velocity, as well as viscous effects based on surface friction. The local forces are then integrated to determine the aerodynamic coefficients. A simplified

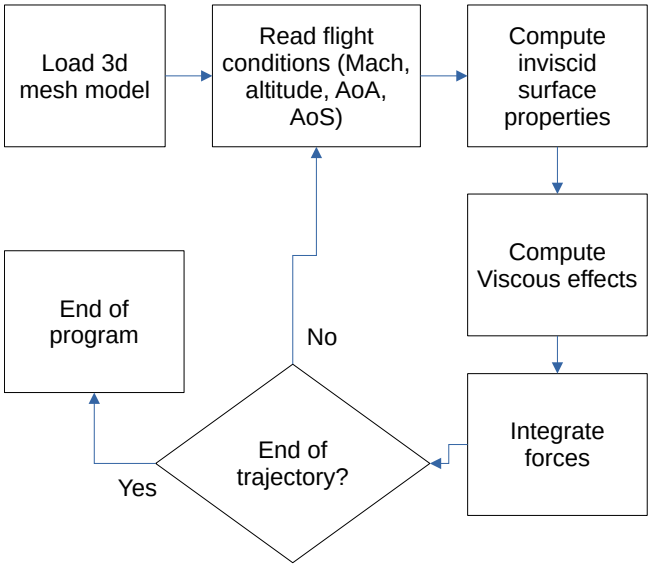


Fig. 1 Computational workflow for HipeX trajectory analysis.

workflow is presented in Figure 1, while detailed descriptions of the numerical models are provided in Subsections 2.1 and 2.2.

The solver, HipeX, processes unstructured surface meshes provided in the Standard Triangulation Language (STL) format. Topological information, such as panel adjacency, is precomputed and cached to significantly accelerate aerodynamic coefficient calculations across varying angles of attack. Atmospheric properties, including pressure, density, and temperature, are determined as a function of altitude using an atmospheric model.

Wall shear stress and surface friction are modeled using Eckert's reference enthalpy method, applicable to both laminar and turbulent boundary layers. The local Reynolds number is evaluated based on the distance from the panel to the estimated leading edge along a streamline. Upon reaching the critical Reynolds number, the transition from laminar to turbulent flow is triggered. The surface heat flux is then derived from the computed skin friction coefficient using the Reynolds analogy.

To enhance computational efficiency, HipeX enables the parallel execution of multiple test cases under varying flight conditions. Each case accounts for a specific set of parameters, including angle of attack, sideslip angle, altitude, and Mach number. This capability can be leveraged to construct comprehensive aerodynamic databases or to simulate complex flight trajectories. Following the computation, the resulting surface distributions of aerodynamic pressure and convective heat flux are exported in the Visualization Toolkit (VTK) file format for post-processing and visualization.

2.1 3D Shock Expansion Method

The shock-expansion method employed here is based on local surface inclination techniques, notably the tangent-wedge approach [8]. These methods rely solely on the local inclination angle to determine whether the flow is undergoing compression or expansion, from which the pressure coefficient is subsequently derived. In the tangent-wedge method, aerodynamic properties over a given panel are computed by assuming an oblique shock forms from the interaction between the panel and the incident free-stream. In this mode, each panel is treated independently. In contrast, the shock-expansion method incorporates the flow conditions resulting from upstream panels when determining the pressure and thermal loads on downstream panels. A known limitation of both methods is that they neglect reflected shock waves, which limits their applicability in regions with complex shock interactions. The pressure coefficient (C_p) used throughout this analysis is defined as:

$$C_p = \frac{P_w - P_\infty}{0.5\ \rho_\infty\ u_\infty^2}, \tag{1}$$

where P_w is the wall (local surface) pressure, P_∞, ρ_∞, u_∞ are the free-stream pressure, density and velocity, respectively. According to the inclination of the panel, the appropriate methodology is selected to compute the flow properties. If the shock wave is not attached to the panel, the modified Newtonian method is used [8], which computes the pressure coefficient using:

$$C_p = C_{p,max} \sin^2 \theta, \tag{2}$$

where θ is the local inclination angle of the panel relative to the free-stream direction. The maximum pressure coefficient $C_{p,max}$ is given by:

$$C_{p,max} = \frac{2}{\gamma M_1^2} \left(\left[\frac{(\gamma+1)^2 M_1^2}{4\gamma M_1^2 - 2(\gamma-1)} \right]^{\frac{\gamma}{\gamma-1}} \left[\frac{1-\gamma+2\gamma M_1^2}{\gamma+1} \right] - 1 \right), \tag{3}$$

where M_1 is the upstream Mach number, and γ is the specific heat ratio. This method yields better results for blunt vehicles. For attached shocks, the pressure and downstream Mach number after the shockwave (M_2) are obtained by solving the $\beta - \theta - M$ relation:

$$\tan\theta = 2\cot\beta \left[\frac{M_1^2 sin^2\beta - 1}{M_1^2(\gamma + cos2\beta) + 2} \right], \tag{4}$$

where β is the shock wave angle. The Mach number downstream of the shock is given by:

$$M_2 = \frac{1}{\sin(\beta-\theta} \sqrt{\frac{1 + 0.5(\gamma-1)(M_1 \sin\beta)^2}{\gamma(M_1 \sin\beta)^2 - 0.5(\gamma-1)}}. \tag{5}$$

The maximum flow deflection angle max for which the shock remains attached can be estimated as:

$$\beta_{max} = \arccos\left[\frac{\sqrt{(A_1 = \sqrt{A_2 A_3} - M_1^2 + 4)/\gamma}}{2M_1}\right], \tag{6}$$

where $A_1 = 3M^2$, $A_2 = \gamma + 1$ e $A_3 = 8\gamma M^2 + \gamma M^4 - 8M^2 + M^4 + 16$. The Prandtl–Meyer expansion is applied to surfaces with negative deflection angles, corresponding to flow expansion rather than compression [9]. The flow properties downstream of the expansion are calculated using the Prandtl–Meyer function $\nu(M)$, given by:

$$\nu(M) = \sqrt{\frac{\gamma+1}{\gamma-1}} \cdot \tan^{-1}\left(\sqrt{\frac{\gamma-1}{\gamma+1}(M^2-1)}\right) - \tan^{-1}\left(\sqrt{M^2-1}\right). \tag{7}$$

To determine the Mach number after expansion, an iterative method is used to solve $\theta = \nu(M_2) - \nu(M_1)$. The Prandtl–Meyer function has a maximum value, corresponding to the maximum deflection angle before the expansion wave becomes invalid. The maximum turning angle (ν_{max}) is given by:

$$\nu_{\max} = \frac{\pi}{2}\left(\sqrt{\frac{\gamma+1}{\gamma-1}} - 1\right) - \nu(M_1). \tag{8}$$

The Prandtl–Meyer method provides a good representation of the physical phenomena, but it can produce a nonphysical solution if the panel has high inclination angles. To address this limitation and maintain physical consistency and numerical stability, the Prandtl–Meyer method is applied only when the local expansion angle is below 50% of the theoretical maximum deflection angle. This approach ensures reliable pressure and velocity predictions, avoiding spurious results associated with excessive expansion inputs. When it is not possible to solve the Prandtl–Meyer equation, the pressure coefficient is estimated using the Gaubeaud formula [10], given by:

$$Cp = \frac{2}{\gamma M_\infty^2}\left[\left(\frac{2}{\gamma+1}\right)^{1.4}\left(\frac{1}{M_\infty}\right)^{2.8}\left(\frac{2\gamma M_\infty^2 - (\gamma-1)}{\gamma+1}\right) - 1\right]. \tag{9}$$

For each panel an appropriate method is selected. All the implemented methods to estimate the pressure coefficient and the associated flow properties over a panel are summarized in Table 1.

2.2 Viscous model

The HipeX framework assumes the existence of a boundary layer using a compressible similarity solution that accounts for both laminar and turbulent regimes. Compressibility corrections are introduced through the Eckert reference temperature method [11] is employed. The reference temperature T^* is given by:

Table 1 Summary of Methods for Estimating and Flow Properties

Panel Condition	**Method**	**Governing Equation(s)**	**Notes**
Detached shock (blunt body)	Modified Newtonian	Eq. 2	Used for large deflections. Assumes detached shock.
Attached shock (compression)	Oblique Shock Relations	Eq. 4 and 5	Accurate for sharp leading edges and moderate deflections.
Expansion region	Prandtl–Meyer Expansion	Eq. 7	For panels with flow turning away (expansion).
Expansion (empirical)	Gaubeaud Empirical Model	Eq. 9	Used when Prandtl–Meyer solution fails.
Neutral or small inclination	Free-stream assumption	$Cp = 0$	No compression or expansion effects assumed.

$$T^* = T_e \left(0.5 + 0.5\frac{T_w}{T_e} + 0.044 r M^2\right), \tag{10}$$

where T_e is the temperature at the edge of the boundary layer, T_w is the wall temperature, and r is a flow regime-dependent coefficient, $r = Pr^{1/3}$ for turbulent flow and $r = Pr^{1/2}$ for laminar flow where Pr is the Prandtl Number. The local Reynolds number is computed by:

$$Re_x = \frac{\rho_e u_e x_l}{\mu_e}, \tag{11}$$

where x_l is the local distance from the leading edge in the streamline direction, u is the velocity and μ is the viscosity. The skin friction coefficient, C_f, is then calculated depending on the flow regime for incompressible flow:

$$C_f = \frac{0.664}{\sqrt{Re_x}}. \tag{12}$$

Turbulent flow:

$$C_f = \frac{0.451}{ln^2(0.056 \cdot Re_x)}. \tag{13}$$

The compressibility effects can be incorporated through a compressibility factor F_c and a Reynolds number correction F_{re_x}, using the following relation:

$$C_{f,i} = F_c C_f(F_{re_x} Re_x), \tag{14}$$

where $C_{f,i}$ is the compressible skin-friction coefficient. The Eckert reference temperature relation yields the compressibility factors $F_c = T^*/T_e$ and $F_{re_x} = \mu_e T_e/\mu^* T^*$. Although F_c and F_{re_x} could be replaced with alternative compressibility corrections, such as the Meador–Smart or Van Driest formulations the Eckert model provides excellent agreement for flat plates and slender vehicles [12].

The heat flux q_w is estimated by:

$$q_w = St \rho_e u_e C_p (T_{aw} - T_w), \tag{15}$$

where C_p is the specific heat at constant pressure, and T_{aw} is the adiabatic wall temperature and St is the Stanton number:

$$St = \frac{C_f}{2Pr^{2/3}}. \tag{16}$$

The adiabatic wall temperature is given by:

$$T_{aw} = T_e(1 + 0.2rM^2). \tag{17}$$

Transition between laminar and turbulent boundary layers is modeled using a critical Reynolds number, Re_{cr} , determined empirically by [13]:

$$\log_{10}(Re_{cr}) = 6.421 \cdot \exp\left(1.209 \times 10^{-4} \cdot M^{2.642}\right). \tag{18}$$

This transition model allows HipeX to estimate where the flow shifts from laminar to turbulent as a function of Mach number and streamline distance. After this point, the laminar and turbulent boundary layers are blended using the intermittency factor, which ranges from 0 (fully laminar) to 1 (fully turbulent) [3] [5]. The effective skin friction coefficient is calculated using:

$$C_f = \gamma_{it} C_{f_{\text{turbulent}}} + (1 - \gamma_{it}) C_{f_{\text{laminar}}}. \tag{19}$$

The intermittency factor γ_{it} is modeled by:

$$\gamma_{it} = 1 - exp(-\hat{n}\sigma(Re_x - Re_{cr})^2), \tag{20}$$

where the spot production parameter $(\hat{n}\sigma)$ is given by:

$$\hat{n}\sigma = 1.5 \cdot 10^{-11} Tu_\infty^{7/4}(1 + 0.58M^{0.2})^{-2}, \tag{21}$$

and Tu_∞ is the turbulent intensity, assumed to be 0.5%. The same approach is adopted to compute T_{aw}. In addition to convective heat transfer, radiative heat transfer becomes significant in hypersonic flows, especially at high altitudes and for vehicles experiencing strong shock layers. Radiation originates from the high-temperature gas in the shock layer and can contribute notably to the surface heat flux. The net radiative heat flux to the surface is given by:

$$q_{\text{rad}} = \varepsilon\sigma\left(T_{amb}^4 - T_w^4\right). \tag{22}$$

The total surface heat flux becomes the sum of convective and radiative contributions:

$$Qw_{tot} = Qw_{conv} + Qw_{rad}. \tag{23}$$

Under specific conditions, radiative and convective heat fluxes can balance each other such $Qw_{tot} = 0$. This implies that the surface is in thermal equilibrium and experiences no net heat gain or loss. Such a condition may occur in carefully designed thermal protection systems or in high-altitude hypersonic flight where radiative cooling is strong enough to offset convective heating. However, this balance is generally rare and typically requires high surface emissivity and extreme flow conditions.

To evaluate the total thermal load experienced by the vehicle, the local surface heat fluxes are integrated over the wet area of the body. The total heat rate Q_{tot} is calculated by:

$$Q_{tot} = \sum_{i=0}^{n_{panel}} Qw_i A_i, \tag{24}$$

where A_i is the area of panel i. The main steps of the HipeX computational pipeline are summarized as follows:

1. Read the mesh and compute connectivity information;
2. For each condition in the trajectory list:
   (a) Compute the atmospheric conditions at the current flight altitude;
   (b) Rotate the mesh to the current angle of attack;
3. Compute the inviscid surface properties using the shock-expansion method;
4. Compute viscous effects, including boundary layer and surface heat fluxes;
5. Integrate the surface pressure and shear stress to obtain aerodynamic coefficients;
6. Store results and proceed to the next trajectory condition.

3 Aerodynamic predictions

To validate the HipeX framework and assess its predictive accuracy, we employ the HEXAFLY-INT configuration as a benchmark case. HEXAFLY-INT (High-Speed Experimental Flight – International) is an international consortium designed to investigate sustained hypersonic cruise at Mach 7–8 [14]. The vehicle features a blended lifting-body design optimized for high aerodynamic efficiency and thermal protection during high-enthalpy atmospheric flight. The configuration has been extensively studied in wind tunnel experiments and computational simulations, providing a reliable reference for validating aerothermodynamic models.

The physical dimensions and aerodynamic reference values used in this study are as follows: the reference area (S) is 2.52 m^2, the wingspan is 1.24 m, the overall length is 3.29 m, the coordinates of the moment reference center (MRC) are (1.455, 0, 0.12) meters in the x, y, and z directions, respectively [15]. Figure 2 shows a schematic of the HEXAFLY-INT configuration used in this benchmark, including its main geometric characteristics and control surfaces.

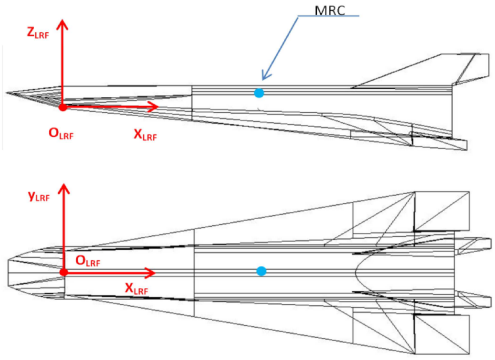


Fig. 2 Drawing of HEXAFLY-INT, adapted from [16].

The results that follow were obtained by using the 1976 U.S. Stander Atmosphere model [17]. Figures 3 and 4 show the aerodynamics coefficients predicted by HipeX compared to CFD results from [18] for M = 7 and M = 6, respectively. HipeX over-predicts the drag at high angles of attack. Under this condition, the boundary layer transition occurs near the rear of the vehicle, resulting in only a small increase in drag for the blended solution compared to the fully laminar solution. In all cases, the predicted position of the center of pressure (X_{cp}) remains within 10% of the CFD data. These results are consistent with previous findings using the tangent-wedge method [6].

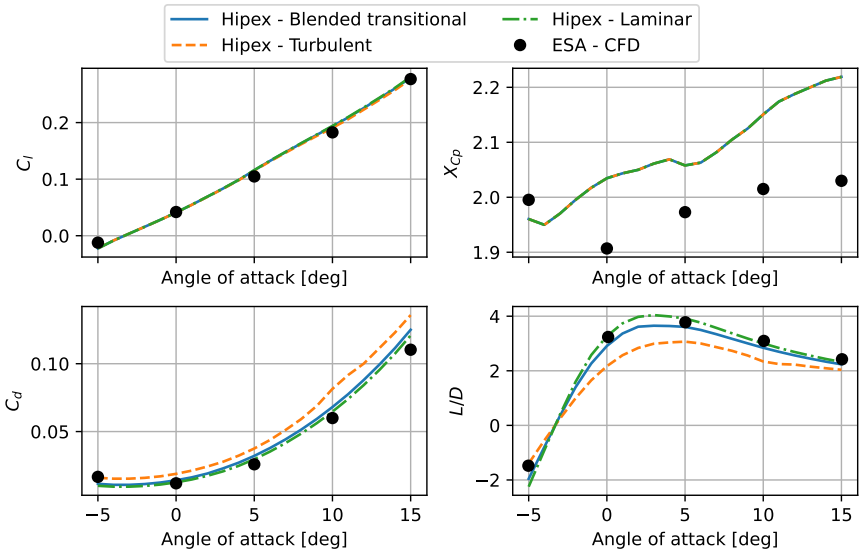


Fig. 3 Comparison of HipeX prediction of aerodynamics coefficients and [18] for M = 7 and 27.9 km of altitude.

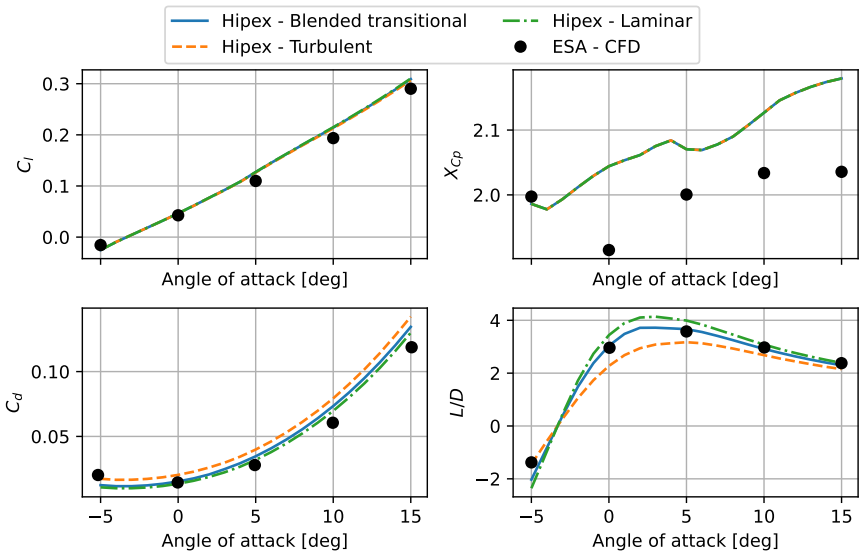


Fig. 4 Comparison of HipeX prediction of aerodynamics coefficients and [18] for M = 6 and 27.6 km of altitude.

For Mach Numbers below 4, the methods implemented in HipeX are know to provide less accurate results. Particularly for $M = 4$, HipeX overpredicts both lift and drag in a proportional manner, resulting in a reasonable agreement in the lift-to-drag ratio (L/D), as shown in Fig. 5. Under this condition, HipeX may still be used with caution to analyze design trends; however, the absolute error in the predicted aerodynamic coefficients can be significant. For $M = 2$, the discrepancies between the CFD results and the HipeX predictions are larger than those observed at higher Mach numbers, as illustrated in Fig. 6. The abrupt changes in the aerodynamic coefficients around an angle of attack of approximately 6 degrees are likely associated with a change in the local flow classification, where surface panels transition between attached and detached shock assumptions. In both cases, HipeX reaches the expected limits of applicability of local surface-inclination methods, which are known to lose accuracy as the flow departs from strongly hypersonic conditions.

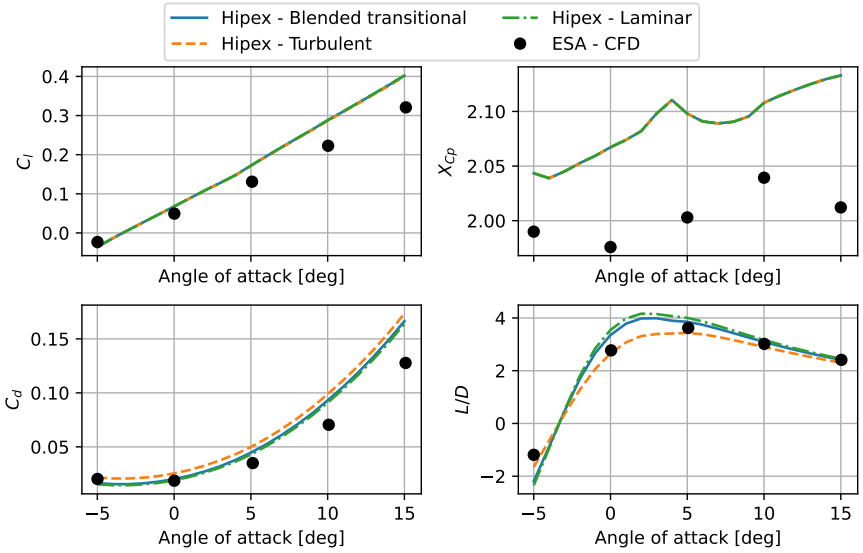


Fig. 5 Comparison of HipeX prediction of aerodynamics coefficients and [18] for M = 4 and 27.2 km of altitude.

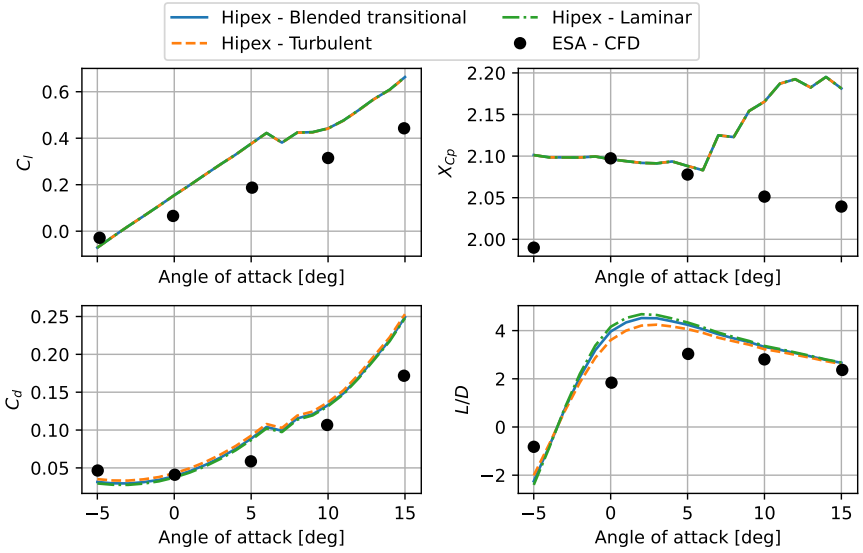


Fig. 6 Comparison of HipeX prediction of aerodynamics coefficients and [18] for M = 2 and 20.3 km of altitude.

The analyzed trajectory, described in Table 2, extends down to Mach 4.8. Along these trajectory points, the aerodynamic efficiency predicted by HipeX using the

blended solution aligns closely with the CFD data from [19] and [20], as shown in Figure 7. At higher altitudes, the flow is predominantly laminar, causing the blended solution to yield results very similar to the fully laminar case. As expected, the blended solution generally provides more accurate results than either the purely laminar or fully turbulent assumptions.

Table 2 Trajectory with critical points [20].

	Tempo [s]	Altitude [m]	Mach	AoA (deg)	sigma(flap)
EFTV-065	273.5	49942	07.07	6.83	-5.46
EFTV-066	288.14	37716.85	7.46	12	-15.44
EFTV-067	290.39	35947.24	7.5	12	-15.39
EFTV-068	294.44	33059.99	7.5	12	-15.38
EFTV-069	300.52	29936.43	7.25	12	-15.72
EFTV-070	305.49	28652.17	7.1	3.62	-2.02
EFTV-071	309.55	28040.09	07.03	1.63	-0.68
EFTV-072	318.37	27461.55	6.88	-0.66	0.41
EFTV-073	350	27444.96	6.42	-1.63	0.64
EFTV-074	500.05	28854.96	4.8	0.51	-2.25

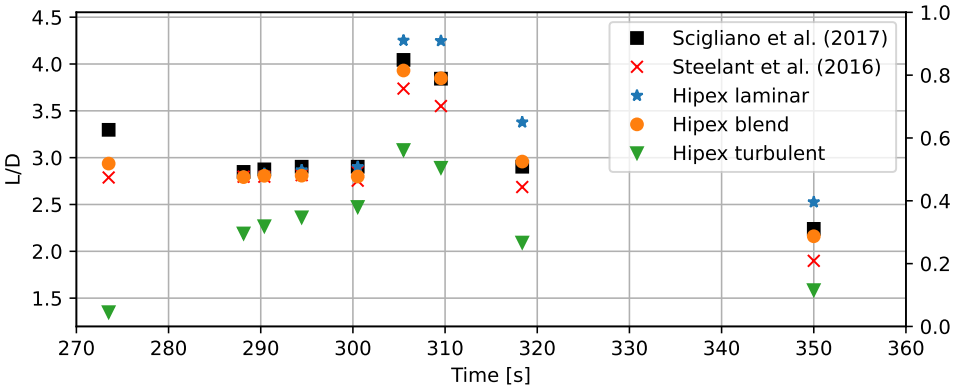


Fig. 7 L/D along the flight trajectory by [20].

Figure 8 shows a comparison of the pressure distribution along the vehicle centerline. Except at the leading edge, the pressure profile predicted by HipeX shows similar behavior to the CFD results. In general, HipeX overpredicts the pressure along the centerline, especially in the nose region. However, the model used in HipeX is simplified by removing the rounded leading edge, resulting in a sharp edge. This geometric difference leads to a pressure peak in the CFD results that is not seen in the HipeX results.

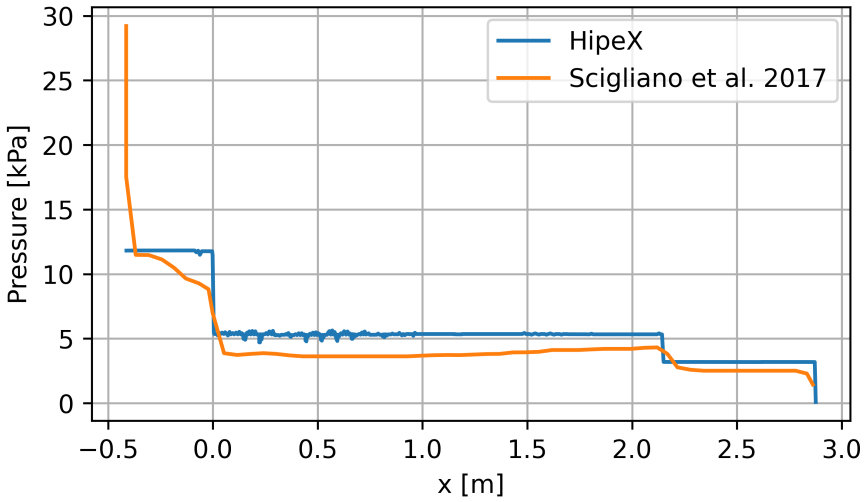


Fig. 8 Pressure distribution for M = 7.5, AoA = 12 degrees and 35.9 km of altitude.

4 Aerodynamic Heating

The surface temperature adopted in the following results corresponds to the equilibrium temperature, defined by the condition where the convective heat flux equals the radiative heat flux. The radiative heat flux is computed assuming an emissivity equal to 0.4. Figure 9 illustrates the surface temperature distribution for Case EFTV-069 in Table 2 and compares the HipeX solution with [21]. For the laminar case at Mach 7.5, altitude 35.9 km, and angle of attack of 12 degrees, the HipeX results are lower than the CFD reference results. The comparison is presented in Figure 10, and corresponds to Case EFTV-067 in Table 2.

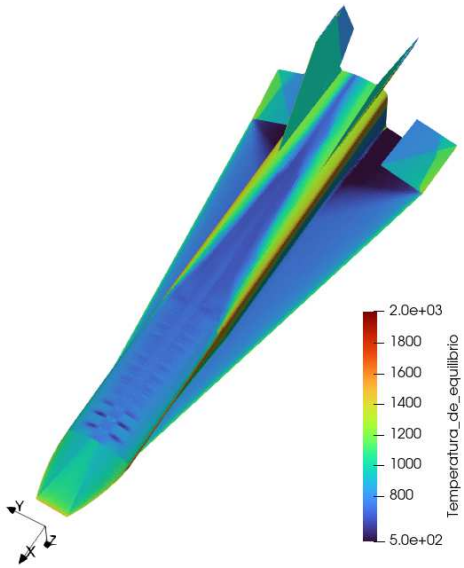


Fig. 9 Radiative equilibrium temperature for M = 7.25 and 29.9 km of altitude.

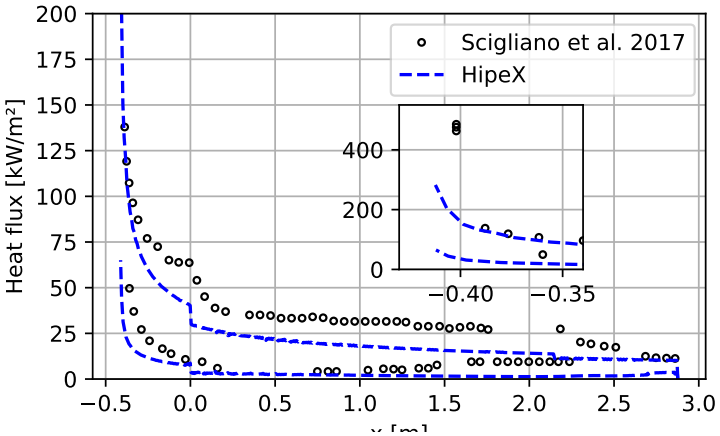


Fig. 10 Heat flux for M = 7.5, AoA = 12 degrees and 35.9 km of altitude, using the laminar solution.

For the case at Mach 7.25, at an altitude of 29.9 km, and at an angle of attack of 12° (EFTV-069), [21] provides heat flux predictions for both laminar and turbulent boundary layer assumptions. The results from HipeX compared with the reference data are shown in Figure 11. The HipeX laminar prediction is slightly lower than the laminar reference data, while the turbulent model slightly overpredicts the heat flux. The blended approach results in a gradual increase in heat flux that bridges the laminar

and turbulent extremes. In HipeX, a turbulent intensity of 0.5% is employed, which directly influences the transition length. This comparison highlights the advantage of the blended approach in providing more realistic and less overly conservative heat transfer estimates.

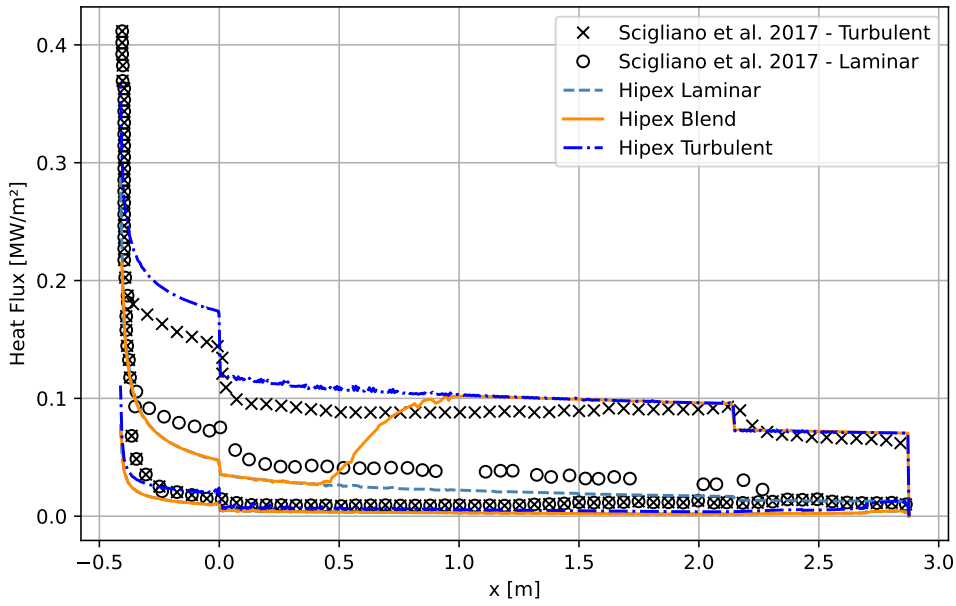


Fig. 11 Centerline heat flux for M = 7.25, altitude = 29.9 km and AoA = 12 degrees.

Figure 12 shows the heat transfer prediction for the case at Mach 6.42, altitude 27.4 km, and an angle of attack of –1.63 degrees (EFTV-073). The HipeX solution is compared with the fully turbulent reference solution from [21]. In this case, the reference heat flux lies between the HipeX laminar and turbulent predictions, indicating that the actual flow is likely transitional. This further reinforces the value of incorporating a blended boundary-layer model to capture the intermediate behavior typical of high-speed flows undergoing natural transition.

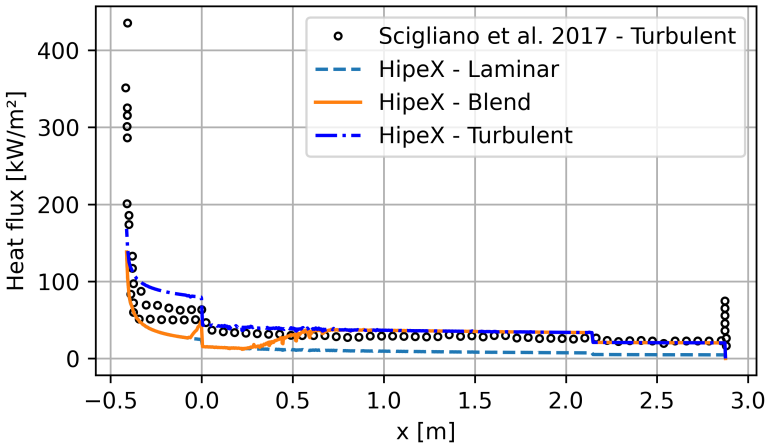


Fig. 12 Centerline heat flux for M = 6.42, altitude = 27.4 km and AoA = -1.63 degrees.

In hypersonic configurations, the region of maximum thermal load typically occurs near the leading edge. Assuming this region to be fully turbulent, as is commonly done in preliminary design, leads to a significant overprediction of heating and, as a consequence, the thermal protection system (TPS) being sized for unrealistically severe conditions. By incorporating a blended transitional model, the solver can capture the fact that the leading-edge boundary layer is often laminar or only partially turbulent along substantial portions of the trajectory. This yields lower and more realistic heat-flux estimates, enabling TPS mass to be reduced without compromising safety margins or mission reliability. The resulting design is less conservative and better aligned with the true aerothermal environment. The main drawback of this approach lies in the inherent difficulty of predicting transition onset in real flight conditions, which depend on surface roughness, freestream disturbances, vehicle vibration, and manufacturing tolerances. Nevertheless, despite this uncertainty, transitional modeling provides a more balanced and physically representative estimate of TPS requirements than assuming fully turbulent flow everywhere.

5 Intermittency comparison

HipeX computes the onset of transition using Equation 20. Figure 13 shows the predicted location of transition onset along the symmetry plane over the reference trajectory from [3]. The results from HipeX and the BLITZ code exhibit similar trends; however, HipeX generally predicts an earlier onset of transition to turbulence compared to BLITZ.

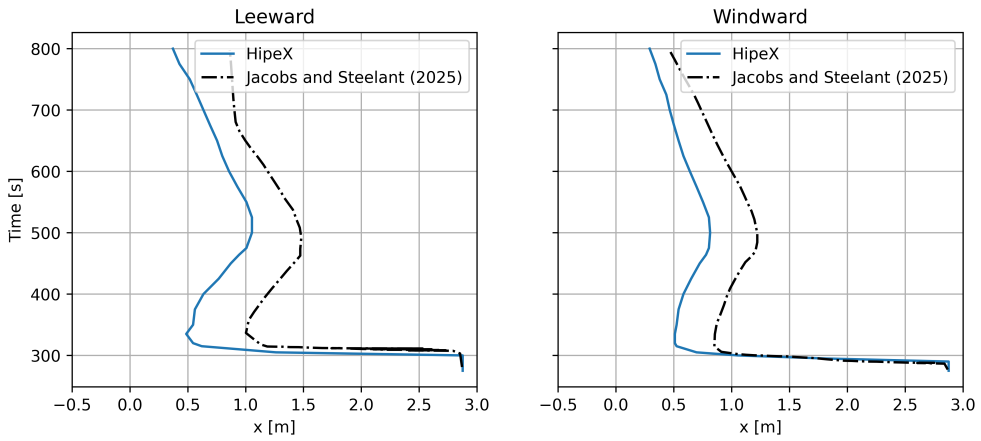
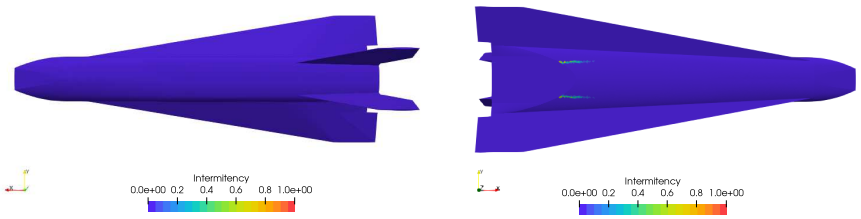


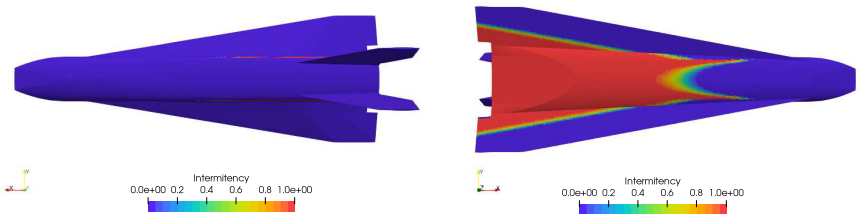
Fig. 13 Location of the beginning of transition at the symmetry plane.

Figure 14 illustrates the intermittency distribution at various time instants along the trajectory. At $t = 290$ s, the flow remains predominantly laminar. By $t = 300$ s, HipeX indicates the development of a turbulent region on the windward side, while the leeward side remains laminar. At $t = 315$ s, a large turbulent region is observed on both the windward and leeward sections. These results are in agreement with Figure 13. Currently, the HipeX model requires further refinement to prevent the prediction of relaminarization in certain expansion regions, as this behavior may not be physically accurate.

T = 290 s, M = 7.5, AoA = 12 degrees and 36.25 km of altitude.



T = 300 s M = 7.28, AoA = 12 degrees and 30.13 km of altitude.



T = 315 s, M = 6.94, AoA = 0 degrees and 27.61 km of altitude.

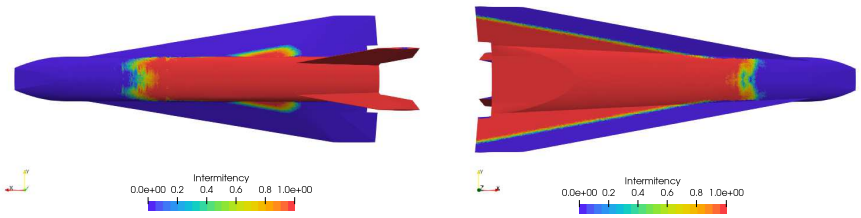


Fig. 14 Intermittency over the Hexafly surface for different instants of trajectory.

6 Conclusion

HipeX demonstrates efficient performance in predicting aerodynamic coefficients with good engineering accuracy and significantly low computational cost. It provides realistic heat-flux estimations for turbulent cases and maintains reasonable trends in transitional regimes, although it tends to under-predict heating under fully laminar assumptions.

The incorporation of a blended transitional boundary-layer model, based on [5], significantly enhances the physical realism of the predictions. This approach captures the partially laminar nature of the leading-edge boundary layer along much of the trajectory, avoiding the overly conservative estimates that result from assuming fully turbulent flow. As a consequence, heat-flux levels are predicted more accurately,

allowing for a reduction in unnecessary thermal protection system (TPS) mass and improving overall vehicle performance by mitigating excessive conservatism common in early design methodologies.

Despite these strengths, HipeX inherits the intrinsic limitations of local surface-inclination methods. The inviscid nature of the underlying models prevents the prediction of shock interactions, separation zones, and strong three-dimensional effects. Furthermore, the accurate determination of transition onset remains challenging in real flight environments. Geometry fidelity can also influence the accuracy of both aerodynamic and thermal predictions.

Nevertheless, HipeX provides a valuable balance between accuracy and computational cost, filling the gap between classical analytical methods and high-fidelity CFD. While ongoing development is still needed, especially regarding transition onset modeling and shock-interaction effects, the current tool already offers a robust foundation for early-stage aerothermodynamic assessment and design of hypersonic vehicles. HipeX enables rapid evaluation of full trajectories and large sets of geometric configurations. For instance, HipeX takes typically one minute to compute the performance of an waverider in a trajectory represented by around 300 points on an i7 workstation with 20 cores, making it especially suitable for preliminary design and optimization tasks.

Acknowledgements. This work was performed within the 'High Speed Experimental Fly Vehicles - International' project fostering International Cooperation on Civil High-Speed Air Transport Research. HEXAFLY-INT, coordinated by ESA-ESTEC, is supported by the EU within the 7th Framework Programme Theme 7 Transport, Contract no.: ACP3-GA-2014-620327. Further info on HEXAFLY-INT can be found on http://www.esa.int/techresources/hexafly_int; the 'Technologies for Hypersonic Flights' project, coordinated by the Institute for Advanced Studies, supported by the Brazilian Funding Agency for Studies and Projects (FINEP) under the Contract no.: 01.22.0255.00, by the Brazilian Air Force (COMAER). This work was carried out with the support of the Academic Cooperation Program in National Defense (PROCAD-DEFENSE), Grant No. 88881.387753/2019-01, and the Conselho Nacional de Desenvolvimento Científico e Tecnológico (CNPq) under Grants No. 307691/2020-9 and 306639/2025-4.

References

[1] Kinney, D.: Aerothermal anchoring of cbaero using high fidelity cfd. In: 45th AIAA Aerospace Sciences Meeting and Exhibit, p. 608 (2007)

[2] Lee, M., Lee, J., Kim, K.H., Kim, H.: Efficient aerodynamic analysis of air-breathing hypersonic vehicle using local surface inclination method based on unstructured meshes. International Journal of Aeronautical and Space Sciences **22**(5), 1031–1041 (2021)

[3] Jacobs, F., Steelant, J.: Impact of transitional boundary layer evolution on slender high-speed flight vehicles. CEAS Space Journal, 1–39 (2025) https://doi.org/10.1007/s12567-025-00639-2

[4] Bertin, J.J., Cummings, R.M.: Critical hypersonic aerothermodynamic phenomena. Annu. Rev. Fluid Mech. **38**(1), 129–157 (2006)

[5] Karsch, M., Eynde, J., Steelant, J.: Linearly combined transition model based on empirical spot growth correlations. CEAS Space Journal **15**(6), 947–958 (2023) https://doi.org/10.1007/s12567-023-00499-8

[6] Araújo, P.P.B., Tanaka, R.Y., Ribeiro, F.H.E., Jr, A.C.F., Passaro, A., Galembeck, L., Camillo, G.P., Jr, D.C., Steelant, J.: Local surface inclination method calculations for the hexafly-int vehicle. In: 3rd International Conference on High-Speed Vehicle Science and Technology (HiSST) (2024)

[7] Rolim, T.C., Cintra, S.C., Pellegrini, M.M.d.C.: Development and application of computational tool using local surface inclination methods for preliminary analysis of hypersonic vehicles. Journal of Aerospace Technology and Management **12**, 2120 (2020)

[8] Anderson, J.D.: Hypersonic and High Temperature Gas Dynamics. Aiaa, ??? (1989)

[9] Anderson, J.D.: Modern compressible flow: With historical perspective (2021)

[10] Guidi, A., Chu, Q.P., Mulder, J.A., Buursink, J.: Implementation of an aerodynamic toolbox in a reentry flight simulator. Journal of Spacecraft and Rockets **40**(1), 138–141 (2003) https://doi.org/10.2514/2.3929

[11] Eckert, E.: Engineering relations for friction and heat transfer to surfaces in high velocity flow. AMER INST AERONAUT ASTRONAUT 1801 ALEXANDER BELL DRIVE, STE 500, RESTON, VA ... (1955). https://doi.org/10.1115/1.4014011 . https://doi.org/10.1115/1.4014011

[12] LANCRY, P.R., WUILBERCQ, R.: Investigation of different skin friction coefficient calculation methods applicable to the design of hypersonic vehicles using mdao approaches. In: 4rd International Conference on High-Speed Vehicle Science and Technology (HiSST) (2025)

[13] Bowcutt, K.G., Anderson, J.D., Capriotti, D.: Viscous optimized hypersonic waveriders. In: 25th AIAA Aerospace Sciences Meeting, p. 272 (1987). https://doi.org/10.2514/6.1987-272 . https://doi.org/10.2514/6.1987-272

[14] Di Benedetto, S., Di Donato, M.P., Schettino, A., Scigliano, R., Nebula, F., Morani, G., Cristillo, D., Marini, M., Cardone, S., Steelant, J., *et al.*: The high-speed experimental flight test vehicle of hexafly-int: a multidisciplinary design. CEAS Space Journal **13**, 291–316 (2021) https://doi.org/10.1007/s12567-020-00341-5

[15] Steelant, J., Villace, V., Kallenbach, A., Wagner, A., Andro, J.-Y., Di Benedetto,

S., Saracoglu, B., Chernyshev, S., Gubanoc, A., Talyzin, V., et al.: Flight testing designs in hexafly-int for high-speed transportation. Proceedings of HiSST (2018)

[16] Brummen, S., Pezzella, G., Andreutti, G., Reimann, B., Steelant, J.: Aerodynamic design analysis of the hexafly-int hypersonic glider. In: 20th AIAA International Space Planes and Hypersonic Systems and Technologies Conference, p. 3644 (2015)

[17] Oceanic, U.S.N., Administration, A., Force, U.S.A.: US Standard Atmosphere, 1976 vol. 76. National Oceanic and Atmospheric Administration, ??? (1976)

[18] Schettino, A., Pezzella, G., Marini, M., Di Benedetto, S., Villace, V.F., Steelant, J., Choudhury, R., Gubanov, A., Voevodenko, N.: Aerodynamic database of the hexafly-int hypersonic glider. CEAS Space Journal **12**, 295–311 (2020) https://doi.org/10.1007/s12567-020-00299-4

[19] Scigliano, R., Pezzella, G., Di Benedetto, S., Marini, M., Steelant, J.: Hexafly-int experimental flight test vehicle (eftv) aero-thermal design. In: ASME International Mechanical Engineering Congress and Exposition, vol. 58349, pp. 001–03022 (2017). https://doi.org/10.1115/imece2017-70392 . American Society of Mechanical Engineers. https://doi.org/10.1115/imece2017-70392

[20] Steelant, J., Villace, V., Marini, M., Pezzella, G., Reimann, B., Chernyshev, S., Gubanov, A., Talyzin, V., Voevodenko, N., Kukshinov, N., et al.: Numerical and experimental research on aerodynamics of a high-speed passenger vehicle within the hexafly-int project. ICAS 2016 Proceedings (2016)

[21] Scigliano, R., Pezzella, G., Marini, M., Benedetto, S.D., Steelant, J.: Aerothermal Design of the Hexafly-int Glider. Aiaa, ??? (2016). https://doi.org/10.2514/6.2016-5627 . https://arc.aiaa.org/doi/abs/10.2514/6.2016-5627